Calhoun: The NPS Institutional Archive

DSpace Repository

Faculty and Researchers | Faculty and Researchers' Publications

1969-10

Experimental Study of Tonks-Dattner Resonances in Rare-Gas Plasmas

Hart, D.A.; Oleson, N.L.

American Institute of Physics

Hart, David Austin, and N. L. Oleson. "Experimental Study of TonksDattner Resonances in RareGas Plasmas." Journal of Applied Physics 40, no. 11 (1969): 4541-4553. http://hdl.handle.net/10945/57632

This publication is a work of the U.S. Government as defined in Title 17, United States Code, Section 101. Copyright protection is not available for this work in the United States.

Downloaded from NPS Archive: Calhoun

http://www.nps.edu/library

Calhoun is the Naval Postgraduate School's public access digital repository for research materials and institutional publications created by the NPS community. Calhoun is named for Professor of Mathematics Guy K. Calhoun, NPS's first appointed -- and published -- scholarly author.

Dudley Knox Library / Naval Postgraduate School
411 Dyer Road / 1 University Circle
Monterey, California USA 93943

Experimental Study of Tonks–Dattner Resonances in Rare-Gas Plasmas

D. A. HART* AND N. L. OLESON†
Department of Physics, Naval Postgraduate School, Monterey, California 93940
(Received 9 June 1969)

Tonks–Dattner resonances were studied in active discharges of neon, argon, and xenon in the milliTorr pressure region where self-excited moving striations are also present. The observed resonance peaks are fewer and broader than have been reported for mercury vapor discharges. The broadening is considerably greater than expected from Landau damping and Coulomb collisions and is attributed to electron density variations associated with moving striations. Direct measurements of electron densities and electron temperatures under resonance conditions permit comparison with the theory of Nickel, Parker, and Gould with no adjustable parameters. The agreement is satisfactory for argon and xenon but the high operating pressure required for stable operation of the neon plasma invalidates the use of the free fall hypothesis and the experimental resonance frequency peaks in this case lie appreciably above the predictions of the theory.

I. INTRODUCTION

When an electromagnetic wave is incident on the positive column of a low pressure discharge with the electric field and the propagation vector both perpendicular to the column axis, multiple peaks are observed in the absorption spectrum of the wave, occurring for frequencies at which the wave is strongly scattered. These resonances were first reported by Tonks[1,2] in 1931. Keeping the frequency constant, he found not only the predicted main dipole resonance but also subsidiary resonances occurring at lower discharge currents. Later these resonances were studied extensively by Dattner[3–6] and others. The subsidiary resonances are now commonly referred to as Tonks–Dattner resonances.

Although several theories of the Tonks–Dattner resonances have been advanced,[7–11] probably the most successful quantitative theory for the resonant oscillations in terms of giving good prediction of the experimentally observed resonant conditions has been presented by Parker, Nickel, and Gould (PNG).[9] The model proposed is one in which finite electron temperatures permit the propagation of longitudinal electron waves of the type described by Bohm and Gross.[12] The observed resonances result from the excitation of standing longitudinal waves trapped in the low density region between the outer edge of the plasma and the position on the radial electron density profile where the electron plasma frequency $\omega_p=(ne^2/m\epsilon_0)^{1/2}$ exceeds the applied frequency ω. A truncated set of moment equations is solved numerically to determine the conditions of resonance. Recently a kinetic model giving a mechanism for the existence of the standing waves has been published by Baldwin and Hirshfield.[13,14] Although the waves propagating in the direction of decreasing electron density are strongly absorbed by Landau damping their model provides a wave moving in the direction of increasing density. This latter wave is formed by those electrons which were previously moving with the phase velocity of the first wave but were reflected by the sheath at the wall.

Most experimental observations of the T–D resonances have been studied using mercury vapor discharges.[9] Despite the fact that the resonances have been observed in a wide variety of gases, very little quantitative data have been reported. The present paper describes experimental studies of T–D resonances in rare gas plasmas, including direct measurements of electron densities and electron temperatures at which the resonances appear in order to permit comparison with the PNG theory with no adjustable parameters.

II. THEORY

A brief resume of the theory of Nickel, Parker, and Gould[9] will be presented here with particular emphasis on its underlying assumptions. The basic equations for a collisionless, non-uniform, electron gas at finite temperatures are employed. Solution of the resulting equation is accomplished by numerical methods.

The fundamental equations used are

$$(\partial F/\partial t)+\mathbf{u}\cdot(\partial F/\partial r)-(e/m)\mathbf{E}\cdot(\partial F/\partial \mathbf{u})=0, \quad (1)$$

$$\mathbf{E}=-\nabla\phi, \quad (2)$$

$$\nabla^2\phi=\rho/\epsilon_0, \quad (3)$$

* Present address: Navy Space Systems Activity, Space Systems Division, Air Force Unit Post Office, Los Angeles, California.
† Present address: Department of Physics, University of South Florida, Tampa, Florida 33620.
[1] L. Tonks, Phys. Rev. **37**, 1458 (1931).
[2] L. Tonks, Phys. Rev. **38**, 1219 (1931).
[3] A. Dattner, Ericsson Technics **2**, 309 (1957).
[4] A. Dattner, *Proc. 5th Int. Conf. on Ionization Phen. in Gases*, Munich, August 1961 (North-Holland Publ. Co., Amsterdam **2**, 1477 (1961).
[5] A. Dattner, Ericsson Technics **1**, 1 (1963).
[6] A. Dattner, Phys. Rev. Lett. **10**, 205 (1963).
[7] W. M. Leavens, Radio Science J. Res. Nat. Bur. Stand. **69D**, 1321 (1965).
[8] F. W. Crawford, Phys. Lett. **5**, 244 (1963).
[9] J. V. Parker, J. C. Nickel, and R. W. Gould, Phys. Fluids **7**, 1489 (1964).
[10] D. E. Baldwin, Phys. Fluids **12**, 279 (1969).
[11] H. N. Ewald, Sperry Rand Research Center, Sudbury, Massachusetts, Report No. 1, October 1968.
[12] D. Bohm and E. P. Gross, Phys. Rev. **75**, 1851, 1864 (1949).
[13] D. E. Baldwin and J. L. Hirschfield, Appl. Phys. Lett. **11**, 175 (1967).
[14] D. E. Baldwin and D. W. Ignat, Phys. Fluids, **12**, 697 (1969).

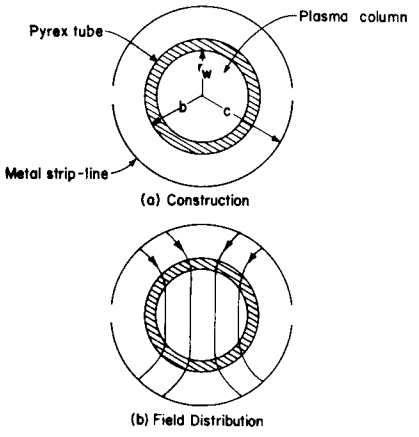

FIG. 1. Split cylinder electrode configuration, (a) construction, (b) electric field distribution.

where $F(\mathbf{r}, \mathbf{u})$ is the electron distribution function, $\mathbf{u}$ and $\mathbf{r}$ being the velocity and position, respectively. The collisionless Boltzmann equation [Eq. (1)] is valid if the frequency of the applied field greatly exceeds the electron-ion and electron-neutral collision frequencies. The ions are assumed to be stationary. Equations (2) and (3) follow from the assumption of the quasi-static approximation which is valid if the free space wavelength of the incident wave is much greater than any lengths of interest such as the discharge tube radius or the Debye length on axis. Solution is effected by taking velocity moments of Eq. (1) and terminating the chain of moments after the second moment. This is equivalent to setting the heat flow equal to zero, a procedure which appears to be valid when $\omega > \omega_p$ where ω is the wave frequency and ω_p the plasma frequency. Such an approach has the consequence that no information is obtained on the effects of Landau type damping on the resonances.

If the further simplifying assumption is made that the electron pressure tensor arising from the second moment can be replaced by a scalar tensor proportional to density, the two moment equations are

$$(\partial n_e/\partial t) + \nabla \cdot (n_e \mathbf{V}) = 0, \tag{4}$$

$$(\partial \mathbf{V}/\partial t) + (\mathbf{V} \cdot \nabla)\mathbf{V} = (1/mn_e)\{-n_e \mid e \mid \mathbf{E} - \nabla p\}, \tag{5}$$

where $\mathbf{V}$ represents the mean velocity of the electrons.

If all quantities are represented as sums of steady state terms (subscript zero) and small perturbations (subscript 1), the variables can be put into the form

$$n_e = n_{e0} f(\mathbf{r}) + n_1(\mathbf{r}) \exp(-i\omega t), \tag{6}$$

$$\phi(\mathbf{r}, t) = \phi_0(\mathbf{r}) + \phi_1(\mathbf{r}) \exp(-i\omega t), \tag{7}$$

$$\mathbf{E} = \mathbf{E}_0 + \mathbf{E}_1 \exp(-i\omega t), \tag{8}$$

$$\mathbf{V} = \mathbf{V}_1(\mathbf{r}) \exp(-i\omega t), \tag{9}$$

where $f(\mathbf{r})$ is a function giving the static spatial variation of the plasma and has the value of unity on axis. If the steady state pressure can be represented by the ideal gas law and the pressure perturbation of the plasma is adiabatic in one dimension ($\gamma = 3$), the electron density is then related to the pressure by

$$p_0 = n_{e0} f(r) K T_e, \tag{10}$$

$$p_1 = \gamma K n_1 T_e. \tag{11}$$

The steady electron velocity distribution is assumed to be Maxwellian so that

$$n_e(r) = n_{e0} \exp[+e\phi_0(r)/KT_e], \tag{12}$$

where n_{e0} is the static electron density on axis.

Substitution of the relations given above in Eqs. (4) and (5) and neglecting drift motions leads to a fourth order partial differential equation in ϕ_1, the perturbation electrical potential

$$\nabla^2\nabla^2\phi_1 - \gamma^{-1}\left(\frac{\nabla f}{f} \cdot \nabla\right)\nabla^2\phi_1 + \left[(\gamma\lambda_{D0}^2)^{-1}\left(\frac{\omega^2}{\omega_{p0}^2} - f\right) - \gamma^{-1}\nabla \cdot \left(\frac{\nabla f}{f}\right)\right] \times \nabla^2\phi_1 - \gamma^{-1}\nabla f \cdot \nabla\phi_1 = 0. \tag{13}$$

The substitution $\phi_1(r, \theta) = \Phi_m(r) \exp(im\theta)$ results in a fourth order equation where the angular dependence has been separated out. If the equation is then put into a dimensionless form by introducing $z = r/r_w$, where r_w

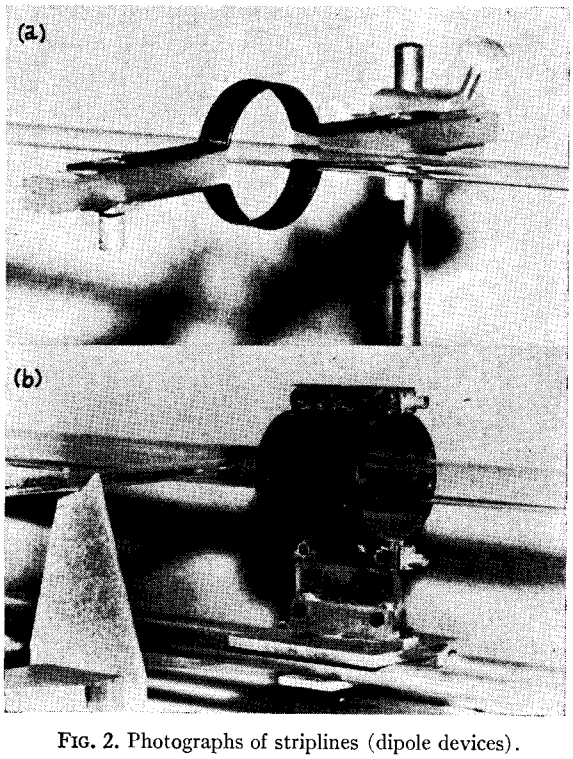

FIG. 2. Photographs of striplines (dipole devices).

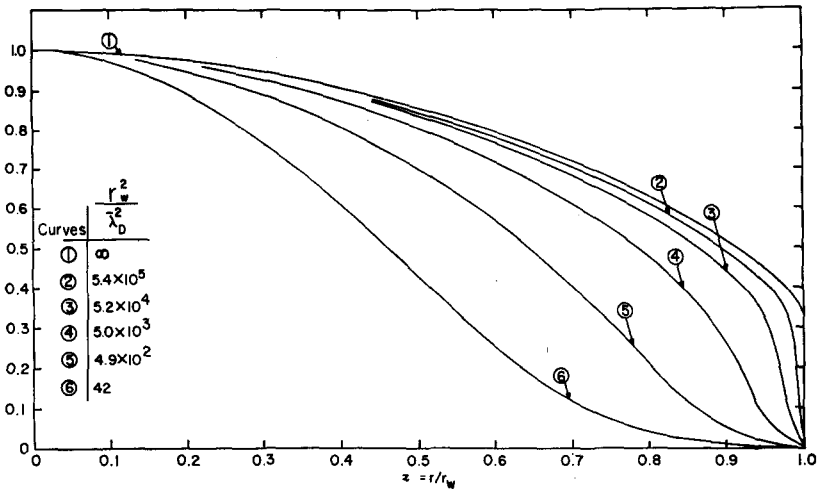

FIG. 3. Theoretical radial electron density profile for argon. That for mercury is very similar.

is the wall radius, the solutions are found to depend only on the dimensionless variables r_w^2/λ_{D0}^2 and ω^2/ω_{p0}^2, where λ_{D0} and ω_{p0} are the Debye length and electron plasma frequency at the center of the column respectively. λ_{D0} is given by $(\epsilon_0 KT_e/n_{e0}e^2)^{1/2}$.

Nickel[9,15] has derived the resonance conditions for an electrode configuration designed to excite a dipolar mode of oscillation in the plasma column. Shown in Fig. 1 is a split cylinder and the electric field configuration used in the present investigation. Figure 2 is a photograph of the assembly. Resonance is considered to arise when the applied electric field approaches zero while the scattered field remains finite, i.e., for poles of the scattering amplitude. The effects of the glass tube and the space between the dipole device and the tube wall are to modify the effective dielectric constant of the medium surrounding the plasma. The resonance condition depends on the experimental apparatus as well as the perturbed electric potential of the plasma, being given by

$$L_m = -mK_{\text{eff}}, \tag{14}$$

where L_m is the logarithmic derivative of the electric potential and is defined by

$$L_m = [(r/\Phi_m)(d\Phi_m/dr)]_{r=r_w} = \Phi_m'(z=1)/\Phi_m(z=1), \tag{15}$$

where m indicates the angular dependence $\exp(im\theta)$. K_{eff} is the effective dielectric constant of the medium surrounding the plasma and is found from

$$K_{\text{eff}} = K\,\frac{(b/r_w)^m(K+g)-(r_w/b)^m(K-g)}{(b/r_w)^m(K+g)+(r_w/b)^m(K-g)}, \tag{16}$$

where K is the relative dielectric constant of the glass walls of the discharge tube and g measures the effect of the split metal cylinder, being given by

$$g = \frac{[1+(b/c)]^{2m}}{[1-(b/c)]^{2m}} \tag{17}$$

and approaches unity when c becomes very large (see Fig. 1).

For dipole type resonances, which should be the mode primarily excited by the split cylinder, $m=1$. When interpreting wave guide data the assumption is made that the electric field is the same as if applied from a split cylinder (strip line) of infinite radius, i.e., $K_{\text{eff}} = K_{\text{eff}}(K, r_w, b, c=\infty)$.

In order to solve Eq. (13), the density profile function $f(r)$ must be known. It has been calculated theoretically for a variety of gases by Parker.[16] The model used is that of a slightly ionized plasma with the neutral gas considered to be at room temperature. The assumption is made that the ions are created with zero velocity at a rate proportional to the local electron density and move radially to the wall without colliding with neutrals. This is essentially the "free fall" theory of Tonks and Langmuir.[17] Their treatment, however, incorporates the additional requirement that $r_w \gg \lambda_D$. The number of ions created per second per unit volume $S(r)$ is considered to be proportional to the local electron density,

$$S(r) = \alpha n_e, \tag{18}$$

where α is the ionization coefficient. Making use of the Boltzmann relation, Eq. (12), and the above assumptions Parker obtains an integro-differential equation (the plasma sheath equation) in terms of the dimensionless variables η and s, where

$$\eta(r) = -e\phi_0/kT_e, \tag{19}$$

$$s(r) = \alpha(m_i/2kT_e)^{1/2}r, \tag{20}$$

[15] J. C. Nickel, California Institute of Technology Report No. 22, Contract No. 220(50), 1964.

[16] J. V. Parker, Phys. Fluids **6**, 1657 (1963). See also, J. V. Parker, California Institute of Technology Report No. 23, Contract No. 220(50), 1964.

[17] L. Tonks and I. Langmuir, Phys. Rev. **34**, 876 (1929).

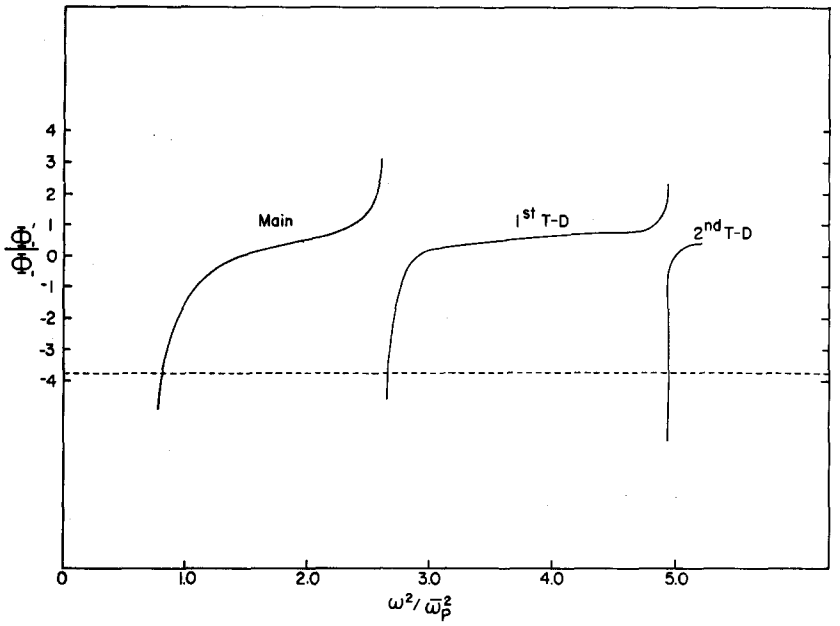

FIG. 4. Logarithmic derivative of dipole potential for $r_w^2/\lambda_D^2=72$. Dashed line at $\Phi'/\Phi=-3.74$ represents the dipole resonance condition, Eq. (14) for $K_{eff}=3.74$.

and the parameter

$$\beta^2=\frac{1}{s_w^2}\left(\frac{r_w^2}{\lambda_{D0}^2}\right)=\frac{n_{e0}}{\bar{n}_e}\cdot\frac{1}{s_w^2}\left(\frac{r_w^2}{\bar{\lambda}_D^2}\right), \tag{21}$$

where $s_w=s(r_w)$. The electron density and Debye length averaged over the radius are given by $\bar{n}_e$and $\bar{\lambda}_D$, respectively.

Numerical solutions of the integro-differential are found for various values of the parameter β^2 making use of the boundary condition that the net *rf* current to the insulated glass tube wall is zero. Solutions for cylindrical geometry for argon in terms of the static radial density function $f(r)=n_e/n_{e0}$ are given in Fig. 3 for various values of $(r_w^2/\bar{\lambda}_D^2)$. The curves for mercury are very similar.

Numerical integration of the perturbation electric potential equation, [Eq. (13)] has been done by Parker[16] using the static theoretical electron density profiles for mercury. The results are given in terms of plots of Φ'/Φ versus $\omega^2/\bar{\omega}_p^2$ where $\bar{\omega}_p^2$ corresponds to the square of the electron plasma frequency value using the average electron density $\langle n_e\rangle$. A typical curve of the sort obtained for mercury is shown in Fig. 4. Other curves for various values of $r_w^2/\bar{\lambda}_D^2$ between 72 and 4530 for both dipole and quadrupole resonance for mercury have been plotted by Parker.[16] From these curves can be obtained the theoretical conditions for dipole resonances. Figure 5 shows the conditions for the main, first and second Tonks–Dattner dipole resonances for $K_{eff}=3.74$, one of the values calculated from Eq. (16), making use of measured values of b and c. The nomenclature of Parker *et al.*[9] has been adopted for the resonances. The largest is labeled the main resonance; subsidiary resonances are numbered in order of appearance from the main resonance, first, second, etc.

Quadrupole resonances have also been observed by Nickel[9,15] using a metallic cylinder constructed of four sections of equal arcs insulated from one another. The alternate sections were driven with opposite polarity to excite quadrupole resonances corresponding to $m=1$ in Eq. (14). No attempt was made to excite quadrupole resonances in the present experiment.

III. DESCRIPTION OF EXPERIMENTS

The Tonks–Dattner resonances in the rare gases were studied at ultrahigh frequencies by employing stripline (dipole device) geometries for a tube of inside radius $r_w=1.56$ cm and by employing stripline and waveguide techniques for a smaller tube $r_w=0.4$ cm (see Fig. 1). The striplines were patterned after those described by Crawford *et al.*[18] but had characteristics identical to the dipole devices used by Nickel.[15] In each case, the stripline diameter was sufficiently larger than the discharge tube diameter to prevent excitation of quadrupole resonances. Discharge tubes were constructed with a hot cathode and after being suitably baked out were filled with spectroscopically pure gas; neon, argon and xenon being used. For striplines, resonances were observed by monitoring radio frequency signals transmitted past the stripline or reflected from it. At the higher frequencies in the microwave region the resonances were detected using the signal reflected from the discharge tube when it was illuminated with radiation from an *S*-band microwave horn which replaced the stripline. In most cases

[18] F. W. Crawford, G. S. Kino, S. A. Self and J. Spalter, J. Appl. Phys. **34**, 2186 (1963).

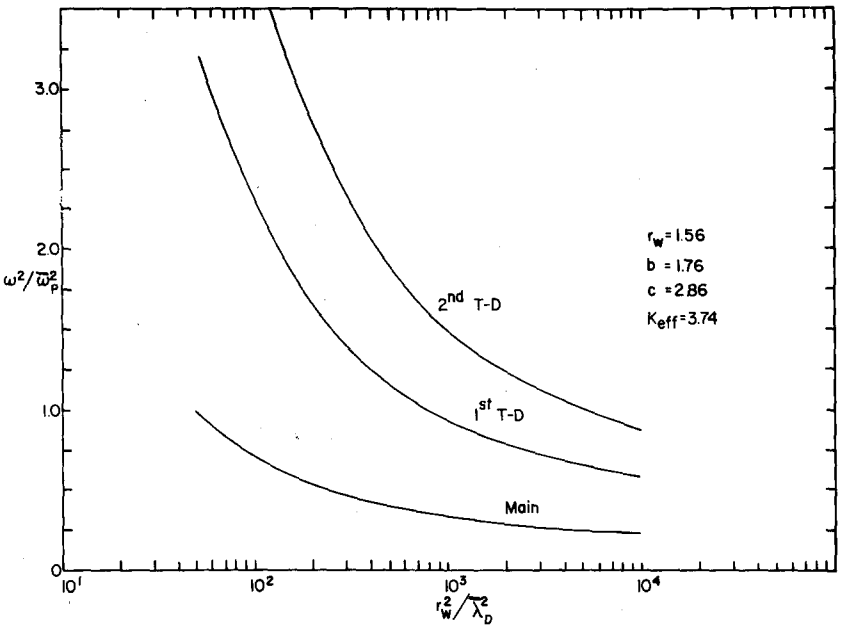

FIG. 5. Theoretical dipole resonance conditions for mercury. Meaning of b and c given in Fig. 1.

observations were made by holding the frequency constant while varying the discharge tube current and thus the electron density. Probe measurements in the larger tube showed that in the range of currents used, the electron density varied linearly with current. No external magnetic fields were applied to the plasma. A diagram of the experimental arrangement using striplines is shown in Fig. 6.

Electron densities in the plasma column of the smaller tube were calculated from the resonant frequency shift of a microwave cavity excited in the TM_{010} mode. Densities so obtained are averages over the plasma cross section. In the larger tube the densities were determined from the ion saturation currents of Langmuir probes, employing the numerical calculations of Chen[19] for zero ion energies.[20] Electron temperatures in both tubes were obtained from Langmuir probe plots. Except in the afterglow,[21] a significant feature of the T–D resonances observed in the rare gases is the appearance of fewer and broader resonances than found in mercury plasmas. This has been noted also by other

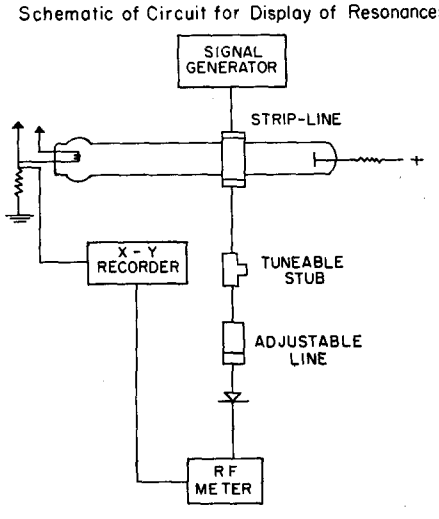

FIG. 6. Circuit for display of resonances using a stripline.

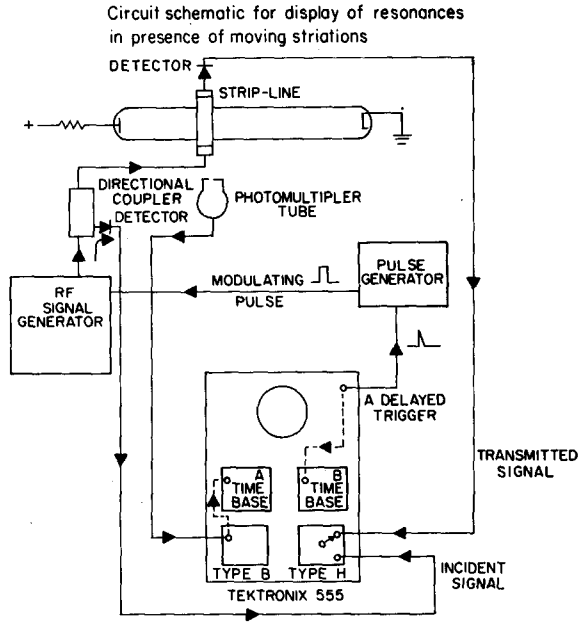

FIG. 7. Experimental arrangement for observation of resonances at various phases of moving striation.

[19] F. F. Chen, Plasma Phys. (J. Nucl. Energy, Part C) **7**, 47 (1965).
[20] D. A. Hart and N. L. Oleson, Phys. Fluids **11**, 1101 (1968).
[21] H. J. Schmitt, G. Meltz, and P. J. Freyheit, Phys. Rev. **139**, A1432 (1965).

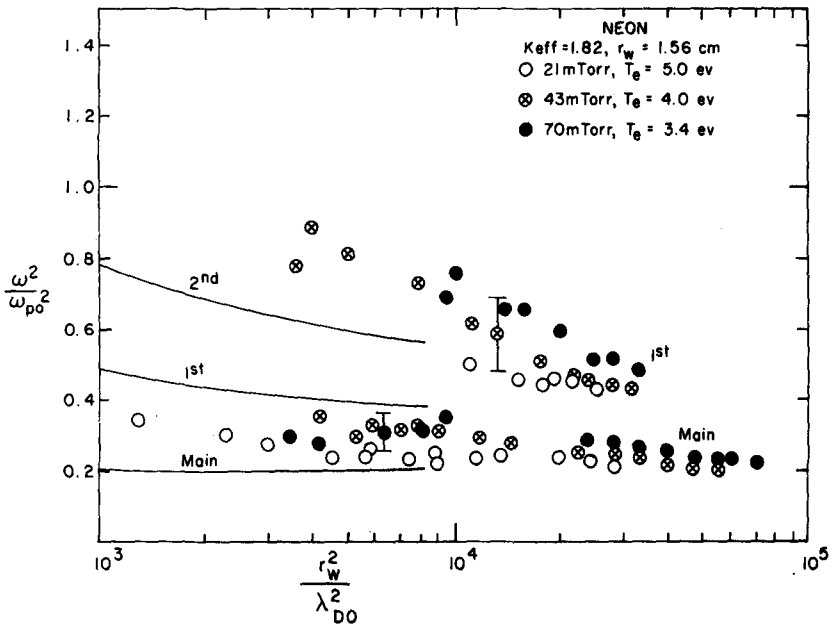

FIG. 8. Dipole resonance spectrum, neon. $K_{eff}=1.82$, $r_w=1.56$ cm, for various electron temperatures and pressures. Solid curve according to theory of Parker, Nickel, and Gould (PNG).

workers.[22–24] In the present experiments in neon and argon only two resonances could be detected at low pressures in the larger tube, between 10 and 100 mTorr in neon and between 1 and 10 mTorr for argon.[25] In each case, only a single broad resonance could be observed above the maximum pressure. The situation was somewhat better in xenon where a total of three resonances could be detected for pressures between about 1 and 4 mTorr. Q's for the resonances ranged from about 2 to slightly over 10, Q being determined from $\omega/\Delta\omega$ where $\Delta\omega$ is the frequency difference necessary to shift the resonance by the width of the half power points. A study of the positive columns of these low pressure electrical discharges showed the presence of low frequency electron density fluctuations which are commonly associated with moving striations.[26] The behavior of the striations was found to be in close agreement with the measurements reported by Alexeff and Jones.[27] The reversal of the phase velocity of the striations was not observed in neon but appeared in argon and xenon at pressures of the same order of magnitude as given by them.

At the lower end of the working pressure ranges cited above the moving striations were of very small amplitude and the corresponding variations of electron density were considered low enough to permit comparison of the observed resonances with the NPG theory. In this comparison average axial densities were used for observations with the larger radius tube ($r_w=1.56$ cm) and average volume densities for the smaller tube ($r_w=0.4$ cm). In order to show the effect of the moving striations on the shape of the resonance peaks, data was also obtained under circumstances such that the resonance measurements were synchronized to different phases of the moving striation wave. For this purpose, the experimental arrangement of Fig. 7 was used.

IV. EXPERIMENTAL RESULTS

In Fig. 8 the results of the experiments for a neon plasma in the larger tube ($r_w=1.56$ cm) are plotted in terms of the dimensionless variables ω^2/ω_{p0}^2 and r_w^2/λ_{D0}^2 where $\omega_{p0}^2=(n_{e0}e^2/m\epsilon_0)$ is calculated from n_{e0} the axial electron density as measured with a Langmuir probe. The Debye length λ_{D0}^2 on axis is calculated using the measured electron temperature, T_e, and the axial electron density. The solid curves represent the theoretical predictions of the *PGN* theory (Sec. II) using these same variables since the numerical data of Parker allow the transformation of theoretical conditions to these quantities.[16] K_{eff} is the effective dielectric constant of the glass and surrounding medium and is given by Eq. (16). Results for several pressures and electron temperatures are shown in this figure.

Similar data obtained for the larger tube in argon and

[22] A. M. Messiaen, Physica **29**, 1117 (1963).
[23] S. Kojima, S. Hagiwara, and H. Ogihara, J. Phys. Soc. (Japan) **20**, 851 (1965).
[24] R. A. Stern, J. Appl. Phys. **34**, 2562 (1963); Appl. Phys. Lett. **4**, 80 (1964); Phys. Rev. Lett. **14**, 538 (1965).
[25] At pressures below about 1 mTorr in argon and xenon and below about 10 mTorr in neon the discharges could not be maintained in the stable normal glow mode. In this region of low pressures the discharge became unstable and the voltage across the discharge no longer remained constant for changing current but arose with increasing current. The current–voltage characteristic was not reproducible and in some cases the discharge changed at random between the normal mode and the unstable mode.
[26] N. L. Oleson and A. W. Cooper, "Moving Striations," Advan. Electron. Electron Phys. **24**, 155 (1968). This is an extensive critical review of this subject covering work published in the past decade.
[27] I. Alexeff and W. D. Jones, Phys. Fluids **9**, 1871 (1966).

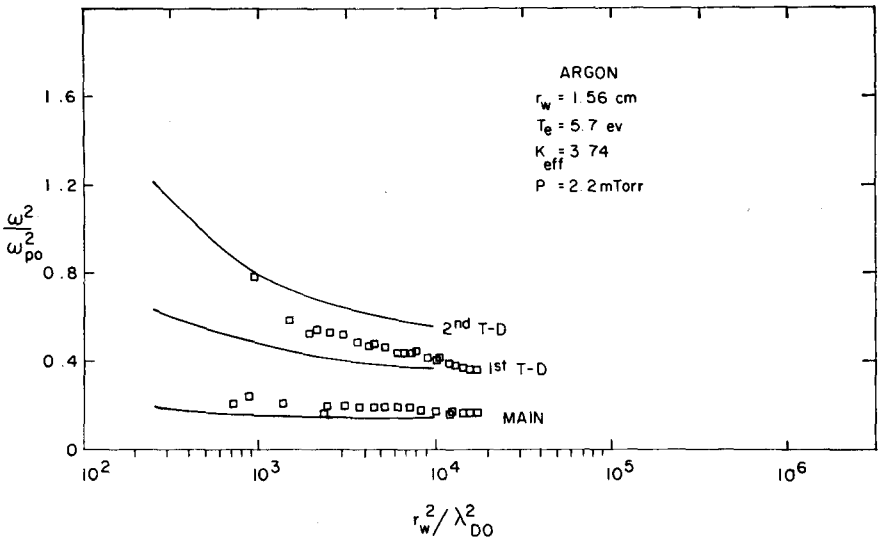

FIG. 9. Dipole resonance spectrum, argon. $K_{eff}=3.74$, $r_w=1.56$ cm, 2.2 mTorr $T_e=5.7$ eV.

xenon plasmas are shown in Figs. 9 and 10, respectively. In Fig. 11 are the results obtained in the smaller tube ($r_w=0.4$ cm) for a xenon plasma. In this figure the variables are defined in terms of the average electron density $\bar{n}$ as measured by a microwave cavity. The data points were taken at several different pressures corresponding to values of T_e ranging from 2.8 to 7 eV and frequencies from 250 MHz to 4 GHz. The group of points shown on the extreme right of the figure was obtained from microwave horn measurements at high discharge currents ($\simeq$500 mA) while the remainder were obtained using a stripline of radius of 2.35 cm. The error flags in Fig. 11 are for the estimated error based on a single measurement. This error is largest at low values of $r_w^2/\bar{\lambda}_D^2$ because of the $\pm$0.3 MHz accuracy with which the cavity resonant frequency can be measured. At high values of the abscissa the estimated error is also large ($\sim$20%) presumably due to reduction in pressure from cleanup resulting from the action of high discharge currents.[28]

As can be seen from Figs. 8–11 the experimental results seem to be in best agreement with the theoretical predictions for xenon and are progressively less so for argon and neon respectively where the resonances appear to occur at higher frequencies than predicted theoretically. Electron temperatures as measured by

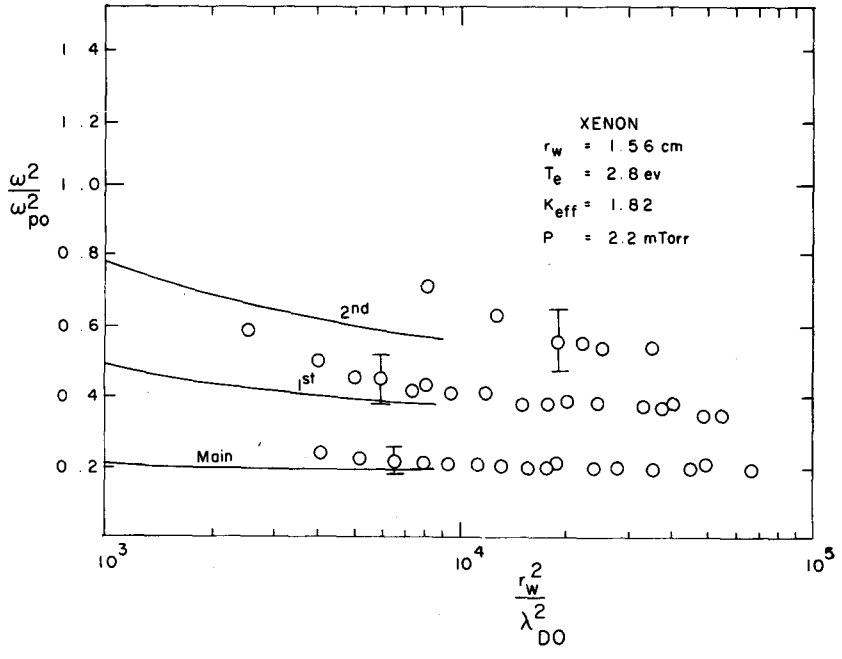

FIG. 10. Dipole resonance spectrum, xenon. $K_{eff}=3.74$, $r_w=1.56$ cm, 1.2 mTorr $T_e=3.6$ eV.

[28] *Scientific Foundations of Vacuum Technique*, J. M. Lafferty Ed. (John Wiley & Sons, Inc., New York, 1962), 2nd ed., p. 665.

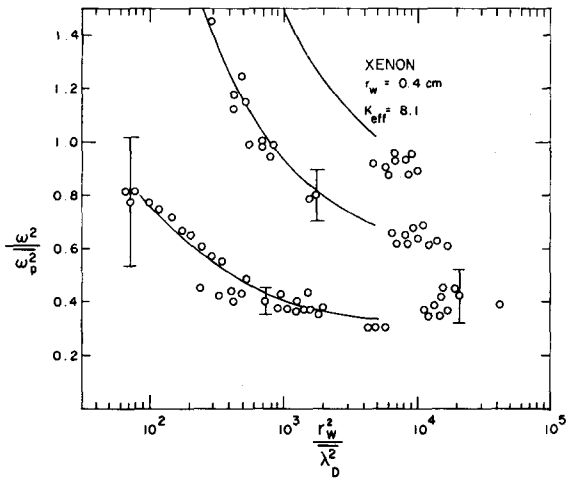

FIG. 11. Dipole resonance spectrum, xenon. $K_{eff}=2.1$, $r_w=0.4$ cm. Three groups of points on right were taken with microwave horn. Variables are defined in terms of average density. Points were taken at several different pressures, this variation being accounted for by inclusion of electron temperature in abcissa. T_e ranged from 2.8 to 7 eV and resonant frequencies from 250 MHz to 4 GHz.

Langmuir probes for the neon, argon, and xenon plasmas are shown as function of pressure in Figs. 12–14. Also shown on these plots are the theoretical electron temperatures predicted from the "free fall" theory[29,30] and the diffusion theory.[31] In the former the ions are assumed to drift to the wall without making collisions whereas in the diffusion theory the electrons are required to make many collisions enroute to the wall, the wall loss being limited by ambipolar diffusion. In Figs. 12 and 13 those portions of the theoretical curves where the basic assumptions of the corresponding theory are not met are shown dashed. In practice the theoretical curves would be linked together by a smooth curve in the intermediate range of pressures where neither theory is valid. The solid curve for xenon shown in Fig. 14 corresponds to the predictions of the free fall theory since in the low mTorr region the operating pressure was low enough to satisfy the requirements of this theory.

Figure 12 shows that the measured values of T_e in neon are appreciably below the predictions of either theory. Pressures required for the stable operation of the neon discharge (21–70 mTorr) were an order of magnitude greater than those for the other two gases. As a result the neon ion-neutral collision mean-free path was considerably less than the discharge tube radius and the basic requirement of the free fall theory was not fulfilled. One of the effects of ion-neutral collisions is to increase the mean lifetime of the ions in the plasma resulting in a decrease of T_e.[29] Higher pressure also result in greater cumulative ionization which can also contribute to the lowering of T_e, particularly at higher values of discharge current, i.e., higher electron densities.

For argon and xenon the agreement with the free fall theory appears to be reasonably satisfactory as shown in Figs. 13 and 14. The operating pressures in these gases were sufficiently low so that the ion mean free path were somewhat greater than the tube radius and the requirements of the free fall theory are more nearly met.

The data given in Figs. 8–11 correspond to an average electron density associated with the presence of moving striations. Figure 15 shows the broad resonance dips

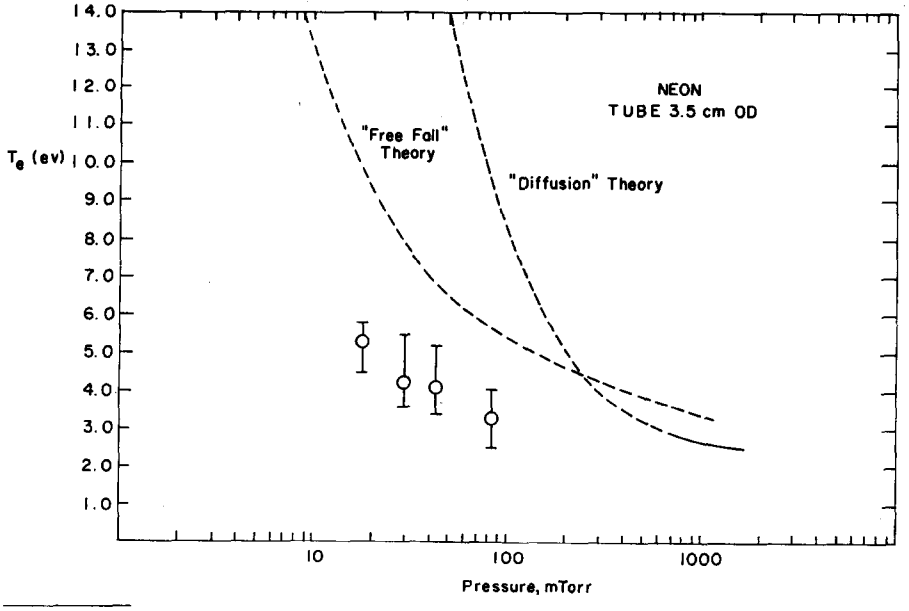

FIG. 12. Electron temperature versus pressure, neon, $r_w=1.56$ cm. Dashed line portions of the curves represent regions where assumptions of the theories are not met.

[29] B. Klarfeld, J. Phys. USSR 5, No. 2–3, 155 (1941).
[30] A. von Engel, *Ionized Gases* (Oxford University Press, New York, 1965), 2nd ed., p. 251.
[31] Reference 30, p. 242.

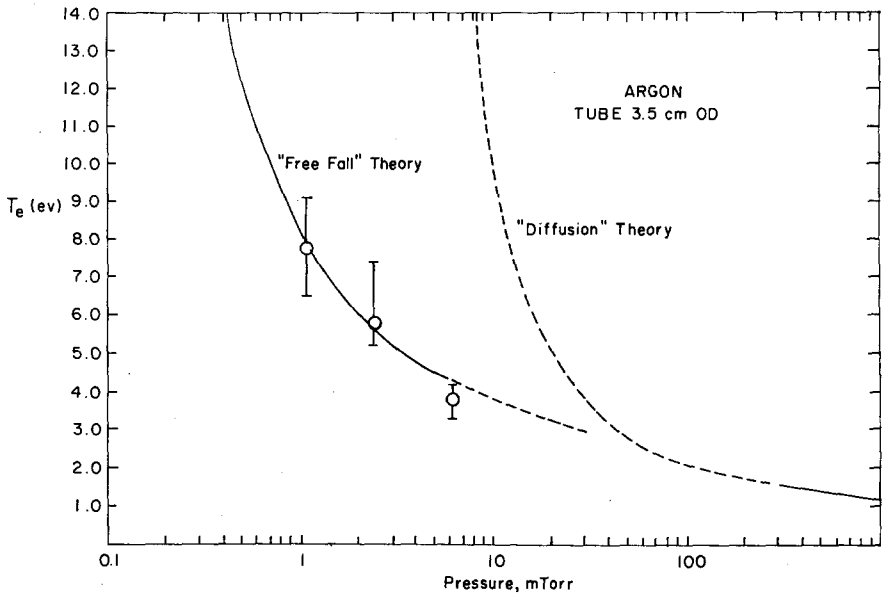

FIG. 13. Electron temperature versus pressure, argon. $r_w = 1.56$ cm. Dashed line portions of curves represent regions where assumptions of theories are not met.

found in the presence of small amplitude moving striations for xenon in the large tube at 1.15 mTorr. Instantaneous measurements at various phases of the striations were also made making use of the circuit shown in Fig. 7. Data are given in Fig. 16 for xenon at 4.3 mTorr of resonance measurements that were synchronized to four different phases of the light intensity variation associated with the moving striation, corresponding to maximum and minimum intensity and two other intermediate phases. For neon at 27 mTorr only resonances at maximum and minimum light intensity were recorded and are given in Fig. 17. In both Fig. 16 and Fig. 17 the resonance at minimum light intensity is observed to occur at lower frequency than that for the corresponding maximum which is to be expected if the minimum light intensity corresponds closely to the minimum of the electron density fluctuation. Within experimental error the resonant frequencies observed in the various phases of the moving striation are those obtained from the corresponding electron densities as found by probe measurements. Electron temperature was found to vary little over the striation cycle. Figures 16 and 17 also reveal that resonances found at minimum light intensity are broader than at the crest of the striations consonant with the fact that the observed light intensity fluctuations had a broad maximum and a rather sharp minimum corresponding to slow and rapid changes of electron density, respectively. In these

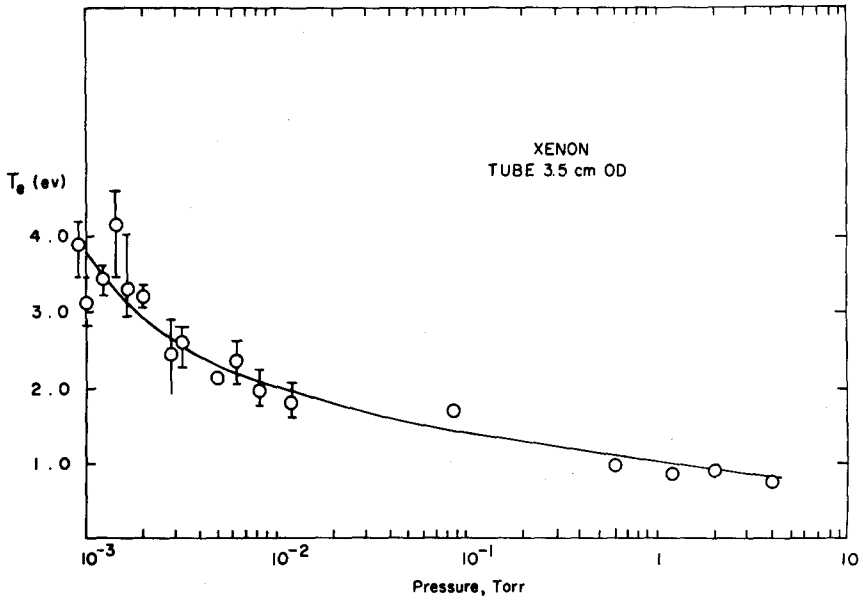

FIG. 14. Electron temperature versus pressure, xenon. $r_w = 1.56$ cm. Solid curve represents predictions of free fall theory. Resonant measurements made only in region where $p \leq 10^{-2}$ Torr.

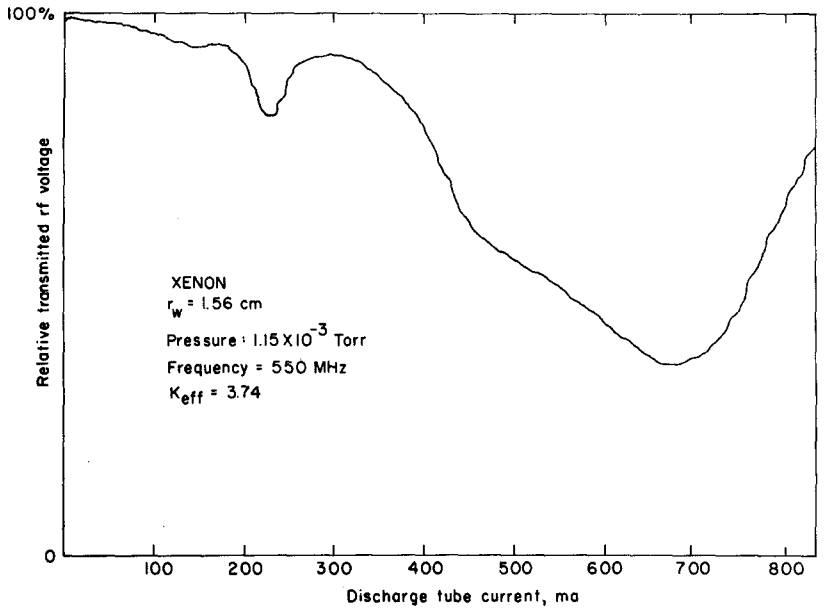

FIG. 15. Resonance in xenon, $r_w=1.56$ cm 1.15 mTorr. Relative transmitted r voltage versus discharge tube current.

instantaneous measurements, contrary to previous procedure, the frequency was varied while the discharge current was kept constant.[32]

V. DISCUSSION OF EXPERIMENTAL DATA

Inspection of the results for resonances shown in Figs. 8–11 indicate that the experimental data agree quite well with the theory of Parker, Nickel and Gould (solid curves) for the case of xenon. However the resonances in argon and neon are observed to occur at higher frequencies than the theoretical predictions, the agreement being worse for neon for which the resonances occur at approximately $\sqrt{2}\times$ the predicted frequencies.

The theoretical curves make use of electron density radial profile calculated by Parker.[16] Although Parker also gives radial profiles for a variety of other gases (but not the resonance conditions for these gases), the influence of ion mass on these profiles is slight. In the case of low density plasmas ($r_w^2/\lambda_p^2 \simeq 10^2$) the departure of the radial profile of neon from that of mercury is greatest for the different ion species studied in the present experiments and an estimate of the influence of the differences in radial profiles on theoretical resonant frequencies has been made. The region in which density variations occur for the Tonks–Dattner resonances is confined between a point near the wall of the tube and a point corresponding approximately to the cutoff of a longitudinal electron wave at the resonant frequency propagating into the plasma from the region near the wall. This cut-off radius can be established for a given resonance occurring in mercury. For neon with the same central density, Parker's results show that the density at this radius will be slightly higher than for mercury.[16] If the assumption is made that the theoretical resonance frequency for the same mode would be shifted upward proportionally to the increase in the square root of the density at this radius, the influence of ion species on the theoretical resonant frequency can be estimated. Using this approach, it is calculated that for the same central density as for mercury the shift in the theoretical ratios of ω^2/ω_p^2 for neon resonances would be increased by about 8% over those of mercury in the worst case, i.e., for $r_w^2/\lambda_D^2 \simeq 10^2$. As the value of this ratio increases to larger values the ion mass has less influence on the theoretical radial profiles and at high values of $r_w^2/\lambda_D^2 (\geq 10^5)$ the difference almost vanishes. Since most of the data taken in the present experiments was obtained for parameters corresponding to $r_w^2/\lambda_D^2 > 10^3$, the theoretical resonance conditions used are considered not inappropriate for the gases to which comparison is made, particularly since experimental error in the electron density measurements is of the order of 10 to 15%. This negligible influence of the ion mass on the theoretical resonance conditions for higher values of r_w^2/λ_D^2 has also been pointed out by Lustig.[33]

If the experimental conditions of the positive column were such that the assumptions of the free fall theory for the radial profiles were not fulfilled the true radial

[32] For measurements of this type to be meaningful, the resonances must be the result of averaging over an axial section of the discharge tube that is small compared to the wavelength of the moving striation. Such a condition was assured by using a narrow (1.5 cm wide) stripline in which the *rf* energy in the field was found to fall off rapidly in both directions along the discharge tube axis. Measurements of the distance between the half power points along the axis of the stripline indicated that the resonance effects corresponded to an averaging over an axial length of the tube of approximately a quarter wavelength of the moving striation. Thus the total instantaneous axial variation of the electron density was reduced to something of the order of 10% for any one measurement.

[33] C. D. Lustig, Phys. Lett. 9, 315 (1964).

profile would not be expected to match the theoretical profile regardless of the question of the influence of ion mass. In all cases the actual radial profiles of the electron density as measured by Langmuir probes failed to reveal any substantial deviation from the free fall profile up to a distance of approximately $0.8r_w$ from the tube axis. Beyond this point the probe had a noticeable perturbing effect and the measurements were considered unreliable. Unfortunately knowledge of the region close to the wall is of vital importance to the understanding of the resonances. The plasma surface wave method recently published by Carlile and Swinford could possible permit determination of the actual radial profile right up to the sheath boundary existing at the tube wall.[34]

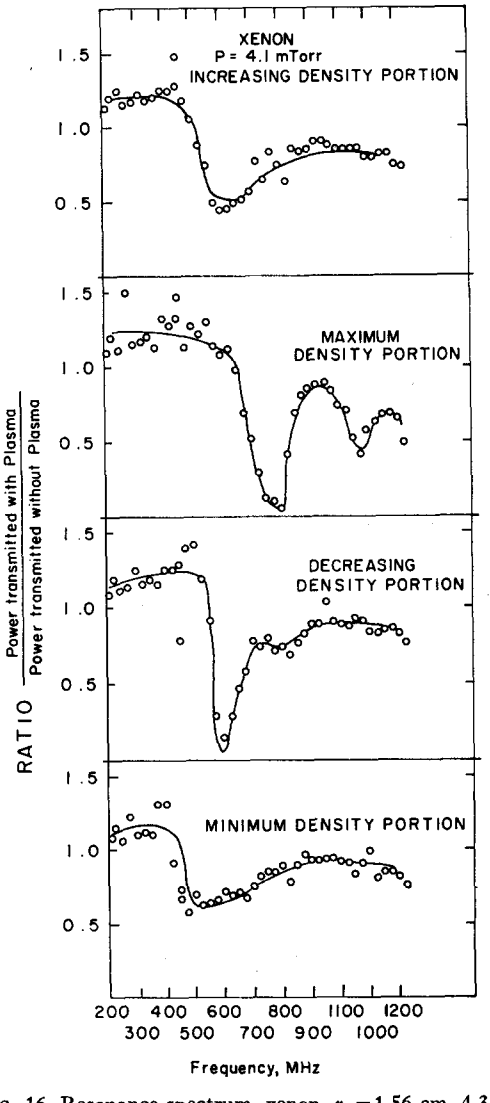

FIG. 16. Resonance spectrum, xenon. $r_w = 1.56$ cm, 4.3 mTorr. Transmitted signal measurements made in synchronization to moving striation phase.

[34] R. N. Carlile and H. W. Swinford, J. Appl. Phys. **39**, 3268 (1968).

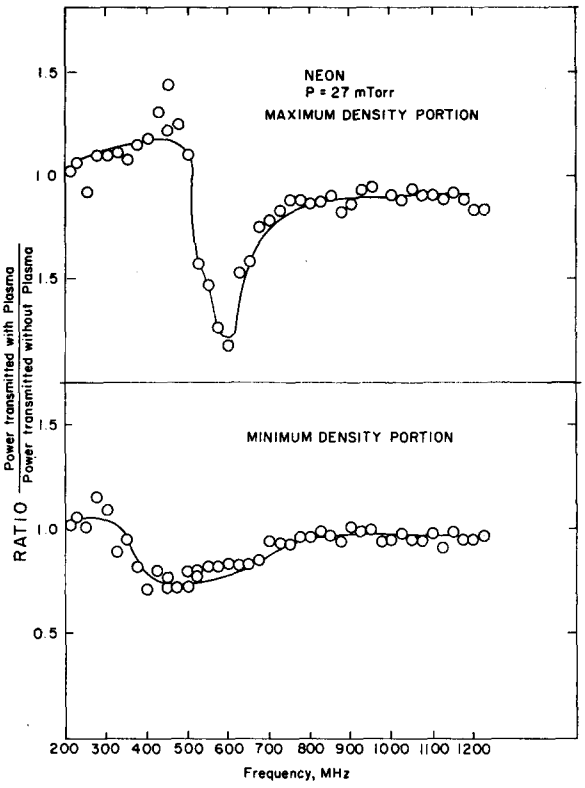

FIG. 17. Resonance spectrum, neon. $r_w = 1.56$ cm, 27 mTorr. Transmitted signal measurement synchronized to moving striation phases corresponding to maximum and minimum light intensity.

As previously pointed out in Sec. IV the high operating pressure required for the neon discharge was an order-of-magnitude higher than required for argon and xenon, resulting in an ion-neutral mean free path small compared to the tube radius. Some additional evidence for the existence of ion collisions in neon is that for successively higher pressures the resonances occur at higher frequencies, indicating a higher density at the wall for the same central density, and as the pressure is lowered the theoretical resonance conditions are more nearly approached. Rough extrapolation of the data for neon in Fig. 8 indicates agreement with the theoretical resonance curve if the pressure is reduced to about 5 mTorr (where stable operation was not possible in neon) at which the ion-neutral free path is calculated to be somewhat greater than the tube radius. To demonstrate this conclusion a plot of the square of the ratio of the observed resonant frequency to that predicted by the PNG theory $(\omega_0/\omega_\eta)^2$ versus the ratio of the tube radius to the ion mean-free path (r_w/λ_i) is shown in Fig. 18. In the limits of large λ_i, the observed resonances are seen to approach the predicted frequencies. Also shown on this plot are some points from the data of Nickel for mercury.[15] All points in Fig. 18 are for values of r_w^2/λ_D^2 of about 10^4.

The observed resonance curves have peaks (or dips) that are extremely broad as shown in Figs. 15–17. In

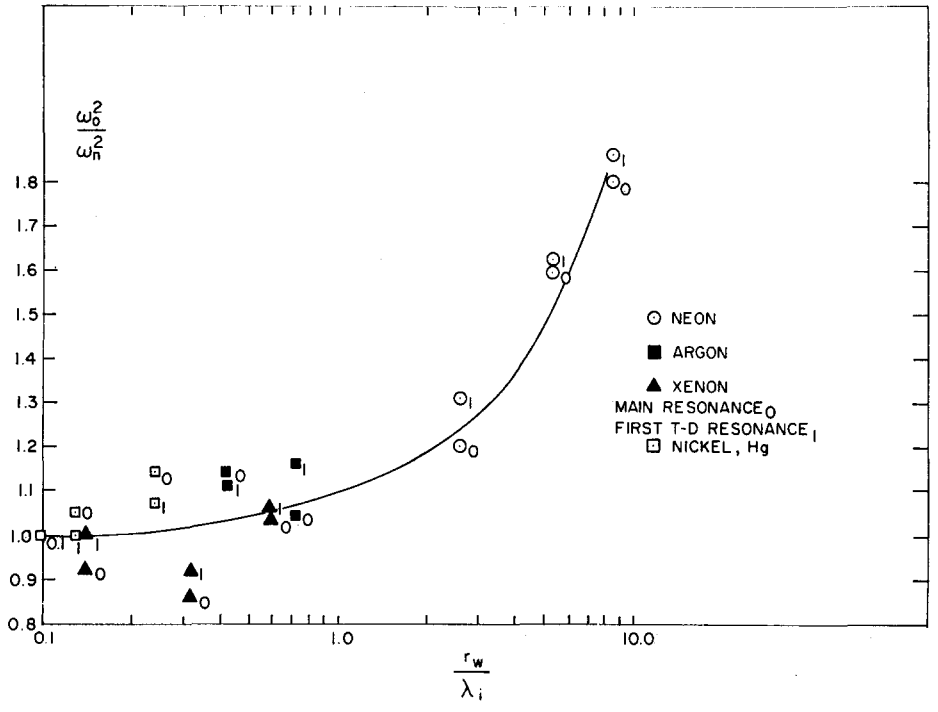

FIG. 18. Plot of square of ratio of observed resonant frequency to theoretical resonant frequency, $(\omega_0/\omega_n)^2$ versus ratio of tube radius to ion mean-free path r_w/λ_i. For large λ_i, the resonances approach the predicted frequencies of PNG theory.

all cases moving striations are present. For the conditions of Fig. 15 a $\pm 50\%$ variation of the electron density, about the average, was observed. Part of this axial density variation is removed by the techniques leading to Figs. 16 and 17, since the transmitted *rf* is sampled only when an axial distance corresponding to approximately a quarter of the striation wavelength is illuminated by the stripline. The result is a reduction of the sampled axial variation to something of the order of 10%. The Q of the resonance observed at the maximum density portion of the striation shown in Fig. 16 is about three times that in which larger density variations occur as in Fig. 15, being about 6.4 and 2.5, respectively.

Even in the circumstances of the synchronized measurements of Fig. 16 the axial density variation can still make an appreciable contribution to the broadening of the resonance peaks, since a 10% axial variation of the electron density is responsible for a line width of about 40 MHz, which is in excess of the broadening due to collision frequencies. The differences in the amount of broadening between the observed resonances at various parts of the striation cycle appear to be accounted for by the differences in the magnitude of the rate of change of density at the corresponding parts of the striation cycle to which the measurements are synchronized. Phototube measurements of the light intensity show that the electron density varies more rapidly in the trough of the striation (minimum light intensity) than at the crest (maximum light intensity) and the observed resonances are broader at the trough than at the crest.

Other possible mechanisms which could contribute to resonance broadening are electron-neutral collisions (and electron-wall collisions), Coulomb type collisions[35,36] and Landau damping.[11,37–39] If the line widths of the synchronized measurements of Figure 16 are corrected for the electron-neutral collision frequency the broadening is still about an order of magnitude greater than predicted by Huggins and Raether[37] as resulting from Coulomb collisions and Landau damping. The extremely broad resonances of the unsynchronized measurements of Fig. 15 are accordingly due to the electron density variations resulting from the passage of moving striations since the accompanying axial density variations of over $\pm 50\%$ of the average density resulting in line widths that are an appreciable fraction of the resonant frequency. This factor alone would seem sufficient to explain the results of Messiaen[22] and Kojima *et al.*[23] whose data showed fewer and broader resonances in the rare gases than have been found in mercury vapor. There is little real evidence of the existence of self excited moving striations in pure mercury discharges.[26] Recently Johnson *et al.*[40] have published a theory on the effect of the interaction of electron density fluctuations and the main dipole resonance and compare their results with experiment

[35] C. L. Chen, Phys. Rev. **135**, A627 (1964).
[36] G. G. Comisar, Phys. Fluids **6**, 76 (1963).
[37] R. W. Huggins and M. Raether, Phys. Rev. Lett. **17**, 745 (1966).
[38] J. F. Decker and C. W. Mendel, Jr., Phys. Rev. Lett. **21**, 206 (1968).
[39] K. J. Harker, G. S. Kino, and D. L. Eitelbach, Phys. Fluids **11**, 425 (1968).
[40] C. D. Johnson, L. A. Berry, and J. C. Nickel, J. Appl. Phys. **39**, 4481 (1968).

for an argon discharge. The fluctuations are found to contribute significantly to the damping.

VI. SUMMARY

Experimental observations of Tonks–Dattner resonances in active, neon, argon and xenon discharges reveal fewer and broader resonances than reported for mercury vapor. For neon, the frequencies of the observed resonances lie considerably above the predictions of the PNG theory. In this case, the operating pressure was such that the ion mean free path was considerably less than the discharge tube radius and the measured electron temperatures were below the predictions of the free fall theory. For argon and xenon, the pressures were low enough so that the corresponding ion mean free path was sufficiently long to more nearly satisfy the requirements of the PNG theory and much less discrepancy between experiment and theory was noted, particularly for xenon.

The broad resonances observed appear to result mainly from the concomitant occurrence of large axial density variations due to the presence of self-excited moving striations. The contributions of these variations and electron-neutral collisions to the broadening is approximately the same and greatly exceed the corresponding contributions from Coulomb collisions and Landau damping.

ACKNOWLEDGMENTS

We wish to thank Professor A. W. Cooper for many helpful discussions. We are also indebted to Mr. H. M. Herreman who was of great assistance in the design of the vacuum systems and who provided many useful suggestions in the course of the experiments. Our thanks are also due to Mr. J. van Gastel for his skillful construction of the glassware and Mr. Peter Wisler for his careful construction of the machined items.

This work was done partly at the Naval Postgraduate School (and supported by the U. S. Office of Naval Research) and partly at the Department of Nuclear Engineering and the Research Laboratory of Electronics, Massachusetts Institute of Technology [supported by the United States Atomic Energy Commission under Contr. AT(30-1)3285].

JOURNAL OF APPLIED PHYSICS VOLUME 40, NUMBER 11 OCTOBER 1969

Electrostatic-Probe Studies in a Flame Plasma

R. M. CLEMENTS* AND P. R. SMY
Department of Electrical Engineering, University of Alberta, Edmonton, Alberta, Canada
(Received 18 December 1968; in final form 26 May 1969)

Simple theoretical considerations have yielded an approximate formula for the ion current per unit length I_i to a cylindrical probe (radius r_p, bias voltage V) immersed in a collision-dominated moving plasma (subsonic velocity $=v_f$, electron density $=n_e$, ion mobility $=\mu_i$).

$$I_i = \frac{2(\pi\mu_i\epsilon_0)^{1/3}(n_e e v_f V)^{2/3}}{[\log(I_i/2n_e e v_f r_p)]^{2/3}} \text{ (mks)},$$

where e is the electronic charge. This relation has been checked with a propane/air flame and a moving probe; it is found to be correct within $\pm 50\%$ over several decades of probe voltage, probe-flame velocity and flame ionization. A more favorable choice of μ_i in the above expression improves the agreement between theory and experiment to $\pm 30\%$. Measurements of sheath thickness obtained from the mutual interference of two adjacent probes support the basic tenets of the theoretical model. It is concluded that, in many instances of probe measurements in flames and other collision-dominated plasmas, the velocity-dependent approach adopted in this paper will be necessary since very large errors can arise if the usual static continuum plasma formulas are used. (Errors of up to a factor of 100 have been reported.)

I. INTRODUCTION

In the study of the kinetic chemistry of ionization of flame plasmas (and in the study of other collision-dominated plasmas), it is often desirable to measure ionization with a high degree of spatial resolution. One of the few techniques which is suitable for such measurements is that of the electrostatic (Langmuir) probe. For a flame plasma at atmospheric density the ion-neutral mean-free paths are much less than the dimensions of any feasible probe with the result that the flow of charges to the probe is collision dominated and is in consequence governed by the appropriate mobility or diffusion constant. Theories have been developed by various workers[1–6] for an electrostatic probe operating

* Now at Department of Physics, University of Victoria, Victoria, B.C., Can.

[1] R. L. F. Boyd, Proc. Phys. Soc. **B64**, 795 (1951).
[2] B. Davydov and L. J. Zmanovskaja, Zh. Tekhn. Fiz. **3**, 715 (1936).
[3] G. J. Schulz and S. C. Brown, Phys. Rev. **98**, 1642 (1955).
[4] C. H. Su and S. H. Lam, Phys. Fluids **6**, 1479 (1963).
[5] C. H. Su and R. E. Kiel, J. Appl. Phys. **37**, 4907 (1966).
[6] I. Cohen, Phys. Fluids **6**, 1492 (1963).